



Study of the Crab Nebula flux variability with the ARGO-YBJ detector

S. VERNETTO¹ ON BEHALF OF THE ARGO-YBJ COLLABORATION

¹INAF-IFSI Torino and INFN Sezione di Torino, Italy

vernetto@to.infn.it

Abstract: The emission of the Crab Nebula has been studied in great detail from radio to gamma ray energies. Thanks to its high flux and stability this source has been considered a standard candle for gamma ray astronomy. An unexpected variability of the gamma ray flux, associated to strong flares, has been recently reported by the AGILE and Fermi collaborations at energies $E > 100$ MeV. In the TeV energy range the source is continuously monitored by the ARGO-YBJ air shower detector, located in Tibet, China, at 4300 m a.s.l. In this paper we report on the observation of the Crab Nebula by ARGO-YBJ during more than 3 years. The results of a search for possible flares on time scales ranging from 1 to 20 days are also presented, with a particular attention to the periods where a flaring emission has been detected by the satellite experiments.

Keywords: Crab Nebula, Pulsar Wind Nebula, Supernova Remnant

The Crab Nebula supernova remnant was observed at very high energies (VHE) for the first time by the Whipple Collaboration in 1989 [1]. A number of different experiments confirmed this detection measuring a VHE spectrum extending up to about 80 TeV [2]. The high flux compared to other known TeV sources and its stability made the source a "standard candle" for VHE gamma-ray astronomy.

The radiation from the Crab Nebula is dominated by non-thermal emission which is attributed to synchrotron radiation from highly relativistic electrons with energies up to $\sim 10^{15}$ eV [3]. The interaction of accelerated electrons with local photon fields (mostly produced by synchrotron emission from the same electron population) can produce VHE gamma-rays via the inverse Compton process [2].

Unexpectedly, on 2010 September 19 the AGILE satellite detected a strong gamma-ray flare from the Crab Nebula direction at energies above 100 MeV [4, 6]. The flare reached its peak during 2 days, with a flux 3 times larger than usual. The event was subsequently confirmed by the Fermi-LAT instrument working in the same energy range [5, 7], and different groups obtained multifrequency data in the following days.

The analysis of the whole Crab data set by AGILE and Fermi showed the presence of a significant gamma ray flux variability during the last years. In particular two strong flares were observed by AGILE in October-November 2007 [6] and by Fermi in February 2009 [7], both lasting 15-20 days. Recently a very intense flare has been detected by Fermi and AGILE on April 2011, with a flux increase of a factor larger than 10 [8, 9].

So far, the origin of this surprising activity is not clear. In this scenario, the observations at TeV energies are extremely important to understand and constrain the mechanisms that produced these unusual events.

In this work we report on the results of the daily observation of the Crab Nebula with the ARGO-YBJ detector performed during 3 years, with a particular attention to the periods characterized by a flaring activity observed by satellite detectors.

1 The ARGO-YBJ experiment

The ARGO-YBJ detector consists of a $\sim 74 \times 78$ m² carpet made of a single layer of Resistive Plate Chambers (RPCs) with $\sim 93\%$ of active area, surrounded by a partially instrumented ($\sim 20\%$) area up to $\sim 100 \times 110$ m². The apparatus has a modular structure, the basic data acquisition element being a cluster (5.7×7.6 m²), made of 12 RPCs (2.8×1.25 m²). Each RPC is read by 80 strips of 6.75×61.8 cm² (the spatial pixels), logically organized in 10 independent pads of 55.6×61.8 cm² which are individually acquired and represent the time pixels of the detector [10]. In addition, in order to extend the dynamical range up to PeV energies, each RPC is equipped with two large size pad (139×123 cm²) to collect the total charge developed by the particle hitting the detector [11]. The full experiment is made of 153 clusters for a total active surface of ~ 6600 m².

ARGO-YBJ operates in two independent acquisition modes: the *shower mode* and the *scaler mode* [12]. In this analysis we refer to the data recorded in shower mode. In this mode, an electronic logic has been implemented to

build an inclusive trigger, based on a time correlation between the pad signals, depending on their relative distance [13]. In this way, all the shower events giving a number of fired pads $N_{pad} \geq N_{trig}$ in the central carpet in a time window of 420 ns generate the trigger. The current trigger condition is $N_{trig} = 20$, corresponding to a rate of ~ 3.5 kHz and a dead time of 4%.

The time and the location of each fired pad are recorded and used to reconstruct the position of the shower core and the arrival direction of the primary particle [14]. The angular resolution and the pointing accuracy of the detector have been evaluated by using the Moon shadow, i.e. the deficit of cosmic rays in the Moon direction [15]. The shape of the shadow provides a measurement of the detector Point Spread Function (PSF), and its position allows the individuation of possible pointing biases. The data have been compared to the results of a Monte Carlo simulating the propagation of cosmic ray in the Earth magnetic fields, the shower development in the atmosphere by using the CORSIKA code [16], and the detector response with a code based on the GEANT package [17]. The measured PSF of cosmic rays has been found in excellent agreement with the Monte Carlo evaluation, confirming the reliability of the simulation procedure.

The Moon Shadow has also been used to check the absolute energy calibration of the detector, by studying the westward shift of the shadow due to the geomagnetic field. The observed displacement as a function of the event multiplicity N_{pad} is also in agreement with the simulation. From this analysis the total absolute energy scale error, including systematics effects, is estimated to be less than 13%.

With the same simulation codes we evaluated the angular resolution for γ rays, that results smaller with respect to protons by ~ 30 -40% depending on N_{pad} , due to the better defined time profile of the showers. In general the PSF can be described by the combination of 2 Gaussian functions. For events with $N_{pad} \geq 40$ (200) the radius of the opening angle that maximizes the signal to background ratio is 1.2° (0.6°) and contains $\sim 55\%$ of the signal.

2 Data analysis

At the ARGO-YBJ site, the Crab Nebula culminates with a zenith angle of 8° and every day is visible for 5.8 hours with a zenith angle less than 40° . The dataset used in this analysis contains all the events recorded from November 2007 to February 2011, with $N_{pad} \geq 20$, where N_{pad} is the number of hit pads on the central carpet. The total on-source time is 5908 hours.

The events are used to fill a set of $8^\circ \times 8^\circ$ sky maps in celestial coordinates (right ascension and declination) with $0.1^\circ \times 0.1^\circ$ bin size, centered on the source position, each map corresponding to a defined N_{pad} interval. We use 8 intervals, corresponding to 20-39, 40-59, 60-99, 100-199, 200-299, 300-499, 500-999 and $>1000 N_{pad}$.

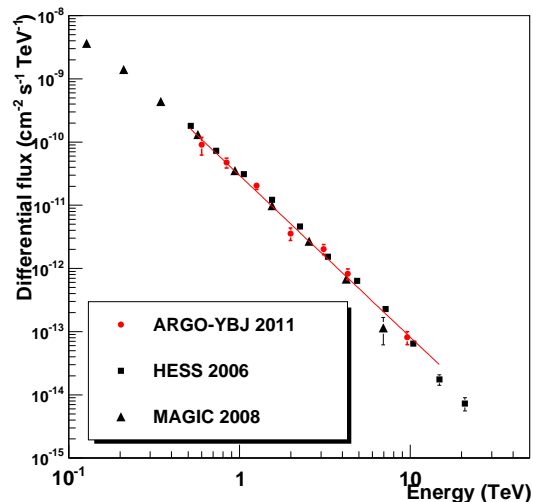


Figure 1: The Crab Nebula spectrum obtained by ARGO-YBJ, compared with other measurements [19, 20]. The reported errors are only statistical.

In order to extract the excess of γ rays, the cosmic ray background is estimated using the *time swapping* method [18] and it is used to build the “background maps”.

The maps are then smoothed using the PSF corresponding to the given N_{pad} intervals. The PSF are obtained by a Monte Carlo procedure that simulates the events from a source with a given spectrum and following a given daily path in the sky. The PSF is weakly dependent on the spectrum slope, that however is known by previous measurements [19, 20]. Finally the smoothed background maps are subtracted to the relative smoothed event maps, obtaining the “signal maps”, where for each bin the statistical significance of the excess is calculated.

An excess at the source position is observed in every map, giving a global significance of 13.5 standard deviations.

The number of events is then corrected taking into account the loss of signal due to the time swapping method, that overestimates the background by a factor depending on the PSF. This correction is larger for small N_{pad} , where the PSF is wider, and ranges from 4% for $N_{pad} > 1000$ to 16% for $N_{pad} = 20$ -40.

The source spectrum is then evaluated by means of a simulation, by comparing the number of excess events for each N_{pad} interval, with the corresponding values expected assuming a set of test spectra. Assuming a power law spectrum, the obtained best fit in the energy range ~ 0.5 -10 TeV is:

$$dN/dE = 3.0 \pm 0.30 \times 10^{-11} E^{-2.59 \pm 0.09} \text{ photons cm}^{-2} \text{ s}^{-1} \text{ TeV}^{-1},$$

with a χ^2 of 8.4 for 5 degrees of freedom.

The quoted errors are purely statistical. We evaluate a systematic error on the flux less than 30% mainly due to the

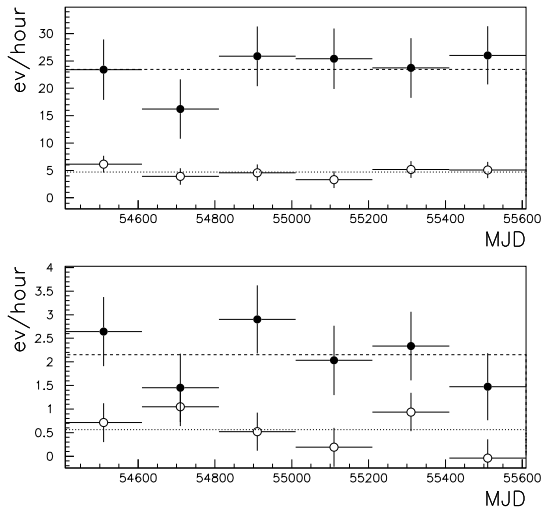


Figure 2: Event rate detected from the Crab Nebula as a function of time, for events with different N_{pad} . Upper panel: $N_{pad} > 40$ and 100 (black and white dots, respectively). Lower panel: $N_{pad} > 500$ and 1000 (black and white dots, respectively).

background evaluation and to the uncertainty on the absolute energy scale.

Fig.1 shows the obtained spectrum, in agreement with previous measurements by other detectors in the same energy range. The energy of each flux point represents the gamma ray median energy in the corresponding N_{pad} interval. These results show the reliability of the ARGO-YBJ measurements in gamma ray astronomy, the stability of the detector and the accuracy of the analysis and simulation procedures.

The Crab Nebula is also used to test possible methods to improve the detector sensitivity. The effects of a selection of showers according to some reconstruction parameters are currently under study. A preliminary result shows that selecting the showers that are spatially more compact and with a smaller dispersion of the arrival time of the particles around the shower front, the cosmic ray background is reduced with respect to gamma rays, giving an increase of the sensitivity by a factor 1.2-1.5, in particular for events with a large number of fired pads. As an example, using this selection for the Crab Nebula events, the significance of the signal increases from 3.7 to 5.1 s.d. for events with 500-999 N_{pad} .

3 Search for flares

The search for possible flares is performed using a data set containing the daily event rates observed from the Crab Nebula. The daily rates are obtained simply counting the excess events per day inside an opening angle of radius Ψ

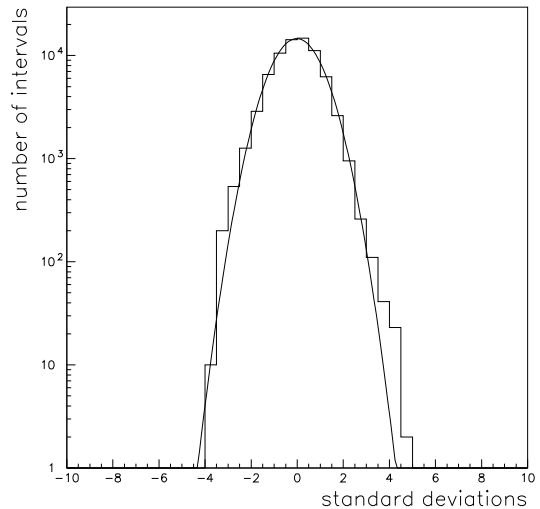


Figure 3: Flare search: distribution of the excesses found for events with $N_{pad} > 40, 100, 500$ and 1000, for 20 flare durations ranging from 1 to 20 days.

around the source, where Ψ is chosen by simulations in order to maximize the signal to noise ratio. In this search the map smoothing according to the PSF is not performed. The rates are evaluated for 4 different N_{pad} thresholds, in order to evidenciate possible variabilities in different energy ranges. We chose $N_{pad} > 40, 100, 500$ and 1000, corresponding to a median energy of $\sim 1, 2, 9$ and 15 TeV. First we study the long-term stability of the source dividing the data in 200 days intervals, and comparing the average rate in each interval with the total average rate. Fig.2 shows that the observed rates are compatible with a constant flux for any of the choosen N_{pad} interval.

To search for flares of duration of the order of hours/days occurred at any time in our data sample, we consider all the intervals of duration $\Delta t = n$ days (with n ranging from 1 to 20) and starting at 00:00 UT each day. For every interval the rate expected from the steady flux is subtracted to the observed rate, obtaining the “flare rates”. The distribution of the significances of the flare rates for the 4 N_{pad} thresholds is given in Fig.3. The number of entries in the distribution is 4×18083 . Note that the excesses are not independent, because the time intervals overlap, and the N_{pad} intervals also overlap. The distribution can be fitted with a Gaussian function, with a mean value $m = -0.021 \pm 0.004$, r.m.s. = 0.983 ± 0.003 , and $\chi^2 = 27$ for 16 d.o.f. The “bump” visible in the distribution for significances larger than 4 standard deviations is due to an excess of 4.6 s.d. with a duration of 15 days, starting on MJD 55030. The excess is observed for events with $N_{pad} > 40$, while for higher N_{pad} thresholds the significance is less than 2 standard deviations. Given the number of trials, the excess chance probability can be estimated of the order of 15%.

A more detailed analysis focused on the time periods where the satellite detectors have observed a flare has been carried out. According to the AGILE and Fermi data [6, 7, 9] three major flaring episodes at energies $E > 100$ MeV occurred during the ARGO-YBJ data acquisition.

Flare 1: starting time MJD 54857, duration $\Delta t \sim 16$ days, maximum flux $F_{max} \sim 5$ times larger than the steady flux [7]. During this flare no excess is present in our data, for any N_{pad} threshold.

Flare 2: starting time MJD 55457, duration $\Delta t \sim 4$ days, maximum flux $F_{max} \sim 5$ times larger than the steady flux [6, 7].

According to the analysis of the Fermi data performed by Balbo *et al.* [21], the gamma ray emission is concentrated in 3 narrow peaks of ~ 12 hours duration each.

We consider the ARGO-YBJ data taken during the 3 transits of the source overlapping the 3 spikes, i.e. the transits on MJD 55457/58, 55459/60 and 55461/62, for a total time of 16.8 hours. By chance, the maxima of the emission occur just during our observation times. Integrating the 3 transits we observe an excess of 3.1 s.d. for $N_{pad} > 40$, while 0.55 s.d. are expected from the steady flux. For higher N_{pad} threshold no significant excess is present. If the excess were due to a flare, the gamma ray flux would be higher by a factor ~ 5 with respect to the steady flux at energies around 1 TeV. Integrating the data over 10 transits (from MJD 55456/57 to MJD 55465/66) the signal significance is 4.1 s.d. (pre-trial), while 1.0 s.d. are expected from the steady flux [22].

No measurement from Cherenkov telescopes are available in coincidence with our observations to confirm this excess. Sporadic measurements performed by MAGIC and VERITAS telescopes at different times from MJD 55456.45 to MJD 55459.49 show no evidence for a flux variability [23, 24].

Flare 3: starting time MJD 55660 [8], duration $\Delta t \sim 9$ days, maximum flux $F_{max} \sim 14$ times larger than the steady flux [9].

Integrating our data over the 6 days in which AGILE detected a flux enhancement, i.e. from MJD 55662.00 to MJD 55668.00, we observe an excess for events with $N_{pad} > 100$ and 500 of significance $\sim 1-2$ standard deviations. Applying the event selection discussed in the previous section, the signal reaches 3.4 and 3.2 standard deviations for $N_{pad} > 100$ and 500, respectively. The signal significances expected from the steady flux in the observation time (34.4 hours) are 0.62 and 0.53, respectively. No measurements from Cherenkov telescopes are available during these days, due to the presence of the Moon during the Crab transits.

4 Conclusions

ARGO-YBJ has continuously monitored the Crab Nebula for more than 3 years. The measured energy spectrum in

the energy range 500 GeV - 10 TeV is in agreement with the results of other experiments.

No flux variations with a statistical significance larger than 5 s.d. have been detected in time scales of days or months. Enhanced flux of significance about 3 s.d. have been observed in coincidence with the occurrence of two flares detected by AGILE and Fermi.

With the current sensitivity, without any gamma-hadron discrimination, ARGO-YBJ can detect in ~ 3 days a flare of intensity ~ 7 Crab units, as the ones observed from the blazar Mrk421 in 2008 and 2010 [25, 26, 27]. Flares of lower intensity are at the limit of the ARGO-YBJ sensitivity.

References

- [1] Weekes, T.C., *et al.* 1989, ApJ 342, 379.
- [2] Aharonian, F.A., *et al.* 2004, ApJ 614, 897.
- [3] Hester, J.J. 2008, Ann. Rev. Astron. Astrophys. 46, 127.
- [4] Tavani, M., *et al.* 2010, Astron. Telegram 2855.
- [5] Buehler, R., *et al.* 2010, Astron. Telegram 2861.
- [6] Tavani, M., *et al.* 2011, Science 331, 736.
- [7] Abdo, A.A. *et al.* 2011, Science 331, 739.
- [8] Buehler, R., *et al.* 2011, Astron. Telegram 3276.
- [9] Striani, E. *et al.*, 2011, arXiv:1105.5028.
- [10] Aielli, G. *et al.* 2006, NIM A, 562, 92.
- [11] Iacovacci, M., *et al.* 2009, Proc. 31st ICRC, Lodz, Poland.
- [12] Aielli, G., *et al.* 2008, Astrop. Phys., 30, 85.
- [13] Aloisio, A., *et al.* 2004, IEEE Transaction on Nuclear Science, 51, 1835.
- [14] Di Sciascio, G., *et al.* 2007, Proc. 30th ICRC, Merida, Mexico (arXiv:0710.1945).
- [15] Di Sciascio, G., *et al.* 2011, these Proceedings.
- [16] Heck, D., Knapp, J., Capdevielle, J.N., Shatz, G., & Thouw, T. 1998, Forschungszentrum Karlsruhe Report No. FZKA 6019.
- [17] GEANT - Detector Description and Simulation Tool 1993, CERN Program Library, W5013.
- [18] Alexandreas, D.E., *et al.* 1993, NIM A, 328, 570.
- [19] Aharonian, F. *et al.* 2008, A&A, 457, 2006, 899.
- [20] Albert, J. *et al.* 2008, ApJ, 674, 1037.
- [21] Balbo, M. *et al.*, 2011, arXiv:1012.3397.
- [22] Aielli, G., *et al.* 2010, Astron. Telegram 2921.
- [23] Mariotti, M., *et al.* 2010, Astron. Telegram 2967.
- [24] Ong, R., *et al.* 2010, Astron. Telegram 2968.
- [25] Aielli, G., *et al.* 2010, ApJL 714, L208.
- [26] Bartoli, B., *et al.* 2011, ApJ, 734, 110.
- [27] He, H.H., *et al.* 2011, these Proceedings.